한국기계가공학회지, 제8권, 제3호, pp 21～26 (2009. 9)
Journal of the Korean Society of Manufacturing Process Engineers, Vol. 8 No. 3, pp. 21～26 (2009. 9)

Analysis of Bulk Metal Forming Process by Reproducing Kernel Particle Method

Kyu-Taek Han#

재생커널입자법을 이용한 체적성형공정의 해석

한규택#

(Received 6 May 2009; received in revised form 21 August 2009; accepted 26 August 2009)

ABSTRACT

The finite element analysis of metal forming processes often fails because of severe mesh distortion at large deformation. As the concept of meshless methods, only nodal point data are used for modeling and solving. As the main feature of these methods, the domain of the problem is represented by a set of nodes, and a finite element mesh is unnecessary. This computational methods reduces time-consuming model generation and refinement effort. It provides a higher rate of convergence than the conventional finite element methods. The displacement shape functions are constructed by the reproducing kernel approximation that satisfies consistency conditions. In this research, A meshless method approach based on the reproducing kernel particle method (RKPM) is applied with metal forming analysis. Numerical examples are analyzed to verify the performance of meshless method for metal forming analysis.

Key Words : Numerical Analysis, Bulk Metal Forming, Reproducing Kernel Particle Method

1. Introduction

In recent years, a new family of computational methods has emerged. The so-called meshless or meshfree methods have been investigated and used by many researchers for treating a large variety of engineering problems, involving usually large displacements as encountered for example in forming process simulations(free surface or moving boundary problems, moving interfaces, cracks propagation, etc.). In these problems accurate finite element solutions require significant computational efforts in remeshing steps. In contrast, meshless methods require only nodal data without explicit connectivity between nodes. The finite element method (FEM), which has been widely used in many engineering problem simulations, exhibits some limitations as the interpolation fails when the elements become too distorted [1-2]. The main advantage of meshless methods is the fact that the interpolation accuracy is not significantly affected by the nodal distribution. However, it is obvious that in any case, an appropriate nodal density is required in order to describe high gradients (boundary layers) as well as an anisotropic behavior

C. A. : School of Mechanical Engineering, Pukyong National University
E-mail: kthan@pknu.ac.kr

of the solution. For this reason, nodal adaptation is needed to compute numerical solutions of problems governed by partial differential equations. In the framework of the finite elements, these adaptation procedures are known as remeshing techniques. Remeshing is required for example when the element geometry becomes too distorted as a consequence of large domain changes. Moreover, sometimes, in order to improve the interpolation accuracy for describing boundary layers or an anisotropic behavior, new nodes must be added, removed or repositioned, and in fact this is not an easy task because the mesh associated to the new nodal distribution cannot contain any too distorted element. If this is not the case, local or global remeshing is required in order to guarantee the geometrical quality of the mesh elements. On the contrary, in meshless techniques, interpolation is free of that mesh requirement. Thus, introduction, eliminations or repositioning of nodes is a trivial task, because no geometrical restrictions exist. In this way, nodes can be added without geometrical checks in the regions where the solution must be improved (identified by using an appropriate error indicator). Once that the new nodes are placed into the domain, and for problems making use of internal variables, these variables can be initialized at those nodes using the standard meshless interpolation. This appealing feature of this kind of techniques simplifies significantly the refinement procedures. In this research, A meshless method approach based on the reproducing kernel particle method (RKPM) is applied to metal forming analysis. Numerical examples are analyzed to verify the performance of the meshless method for metal forming analysis. [3-8]

2. Reproducing kernel particle method

Consider an integral transformation T of a function u.

$$v(x) = Tu = \int_{\Omega} \Phi_a(x-s)u(s)ds \tag{1}$$

where v(x) is the transformation of u(x). If the kernel $\Phi_a(x-s)$ is chosen to be close to $\delta(x-s)$ then $v(x) \rightarrow u(x)$. The kernel function used in this paper is:

$$\Phi_a(x-s) = \frac{1}{a}\phi(\frac{x-s}{a})$$

$$\Phi(z) = \begin{cases} 2/3 - 4(|z|)^2 + 4(|z|)^3 & \text{for } 0 \le |z| \le 1/2 \\ 4/3 - 4(|z|) + 4(|z|)^2 - (4/3)(|z|)^3 & \text{for } 1/2 \le |z| \le 1 \end{cases} \tag{2a}$$

$$0 \quad \text{otherwise} \tag{2b}$$

where $z=(x-s)/a$ and a is the support of the function $\Phi_a(z)$. This estimation is not accurate near the boundaries. Liu et al. corrected the approximation by introducing a modified kernel function $\bar{\Phi}_a$ as follows:

$$u^a(x) = \int_{\Omega} \Phi_a(x;x-s)u(s)ds \tag{3}$$

$$\Phi_a(x;x-s) = C(x;x-s)\Phi_a(x-s) \tag{4}$$

where $u^a(x)$ is called the reproduced function of $u(x)$ and it exactly reproduces N-th order polynomial.

$C(x;x-s)$ is called the correction function and was developed to impose the completeness requirement, and $H(x-s)$ is a vector of polynomial of order N.

$$C(x;x-s) = H^T(0)M^{-1}(x)H^T(x-s) \tag{5}$$

$$H^T(x-s) = \left[1, x-s, (x-s^2), ..., (x-s)^N\right] \tag{6}$$

Applying the trapezoidal rule to Eq.(3) one gets:

$$u^a(x) \equiv \sum_{I=1}^{NP} \Phi_a(x;x-x_I)u(x_I)u(x_I)\Delta x_I = \sum_{I=1}^{NP} \Psi_I(x)u_I, \tag{7}$$

$$\Psi_I(x) = \Phi_a(x;x-x_I)\Delta x_I = H^T(0)M^{-1}(x)H(x-x_I)\Phi_a(x-x_I)\Delta x_I \tag{8}$$

where NP is the total number of particles and Ψ_I's can be interpreted as the shape functions of $u^a(x)$. Since the kernel function Φ_a in Eq.(2b) is $C^2(\Omega_x)$ one can show that Ψ_I is also $C^2(\Omega_x)$. The purpose of discretizing Eq.(3) is to obtain the shape functions, therefore $\triangle x$ in Eqs. (7) and (8) is set to unity for simplicity.

3. Meshless Formulation in Elasto-Plasticity with Contact Conditions

Contact conditions are included to handle contact between tools and workpiece. The classical Coulomb law is used to model frictional contact and the penalty method is applied to assure impenetration. The contact traction's t_n and t_t in the normal and tangential directions, respectively, are defined as follows:

$$t_n = -\alpha_n g_n \tag{9}$$

$$t_t = -\alpha_t g_t \ \ if\ \ |\alpha_t g_t| \le |\mu_f t_n| \ \ (stick\ conditions) \ \ on\ \Gamma^C$$
$$-\mu_f t_n \ \mathrm{sgn}(g_t) \ \ otherwise \ \ (slip\ conditions) \tag{10}$$

where μ is the coefficient of friction, α_n and α_t are the normal and tangential penalty numbers, and g_n and g_t are normal and tangential gaps between contact surfaces. The variational equation of the problem can be written as:

$$\int_x \delta u_{i,j}\tau_{i,j}\,d\Omega - \int_{\Omega_x} \delta u_i b_i\,d\Omega - \int_{\Gamma_x^h} \delta u_i h_i\,d\Gamma + \int_{\Gamma_x^c} (t_n\delta g_n + t_t\delta g_t)\,d\Gamma = 0 \tag{11}$$

The contact term is integrated by collocation formulation to yield

$$\int_{\Gamma_x^c} (t_n\delta g_n + t_t\delta g_t)\,d\Gamma = \sum_A (F_n\delta g_n + F_t\delta g_t)_A \tag{12}$$

where Ω_x is the current domain, $\Gamma_x^h{}_i$ is the current non-contact traction boundary, and $\Gamma_x^c$is the contact boundary, τ_{ij} is the Cauchy stress, b_i is the body force, h_i is the non-contact surface traction, F_n and F_t are the nodal normal and tangential contact forces and A is summed over the contact nodes on the deformable body.

4. Numerical Examples

Two examples of metal forming processes are modeled : cold upsetting and ring compression test. The upsetting process is a basic metal forming operation used in most forging sequences. The ring compression test was developed to experimentally estimate the friction coefficient in metal forming operations. These analysis are good test problems to verify the use of the meshless method as a simulation and design tool for metal forming applications.

4.1 Ring compression process

The test consists of compressing a ring at different ratios with flat and smooth tools and measuring the final height (*hf*) and final internal diameter (*dif*). During compression, the internal and external diameters will change according to the amount of compression and the friction condition of the interface. Hence, curves relating changes in the internal diameter with respect to the compression ratio characterize the coefficient of friction (μ). The ring test was simulated with physical properties of the cold forging steel 16MnCr5, considered as elastic–perfectly-plastic with yield stress σ =100Mpa, Young's modulus *E*=288GPa, and Poisson's ratio ν=0.3. The geometrical dimensions of the ring *deo*:*dio*:*ho* (initial external diameter:initial internal diameter:initial height) are in proportion to 6:3:2. The lubricant used in this test was the bisulfate of molybdenum, which is widely used in cold metal forming processes. Due to the axial and radial symmetries, the simulation was made with one quarter of the ring (discretized with 160 points). In Fig.1(a) the half cross section of the initial ring

model is shown. The kernel support was chosen to cover five points in each direction and the number of time steps was 1000. The prescribed displacement was applied at the master contact points which simulate the flat tool profile. The ring test simulation results for coefficients μ=0 and μ=0.15 shown in Fig.1(b) are in agreement with Male's results. In the case of μ=0.3 and maximum friction, or stick condition, the results are close to Male's. Kernel functions with supports that cover five and seven points are used to study the solution convergence. Basically, with a bigger support the contact surface appears smoother, but the ring profile remains the same.

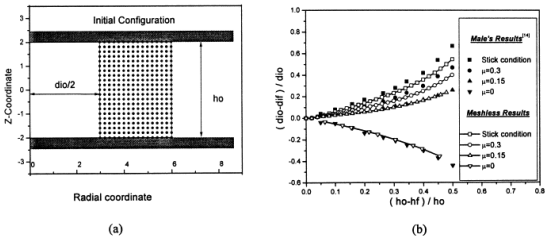

Fig.1 (a) Ring meshless model, (b) ring calibration curves.

4.2 Cold upsetting process

The upsetting process was modeled as shown in Fig.2(a). In this analysis, axisymmetric formulation was used, and prescribed displacement was applied to the punch. The material constants are the as follows: Young's modulus *E*=288GPa, Poisson's ratio ν=0.3 and the material was considered perfectly plastic with yield stress σ =100Mpa. Coulomb friction (μ) between punch and part is estimated from experiments, mainly based on lubrication conditions and tools' finishing surface, and is adopted in the model to be equal to 0.15. The final shape is compared with experimental results in Fig.2(b).

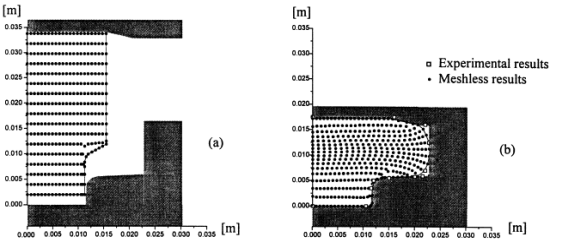

Fig.2 (a)initial and (b)deformed configuration of the upsetting operation.

In this analysis, upsetting operation is successfully simulated by the meshless method without experiencing mesh distortion. Numerical prediction of the final shape of the formed part is in good agreement with the experimental results.

5. Comparison of RKPM and FEM models

Fig.3 presents the computed evolution of the axisymmetric RKPM and FEM models that were used in the numerical analysis of the process. The agreement between the profiles predicted by RKPM and FEM is excellent.

The plane-strain models were set-up at the mid-length cross section of the bars and the remaining numerical conditions were similar to those employed in the previous case. Fig.4 presents

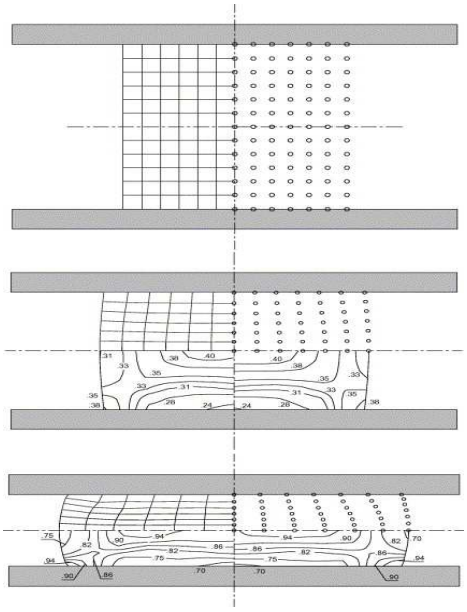

Fig.3 Computed evolution of the compression of cylindrical preforms at different stages of deformation obtained from FEM (left) and RKPM (right): initial shape, 28% and 57% reduction in height. Mid and bottom figures also include the effective strain distribution predicted by RKPM and FEM.

the computed evolution of the RKPM and FEM models that were used in the analysis of the process as well as the predicted distribution of effective strain at 50% height reduction. The agreement is very good.

6. Conclusion

This study presented a thorough description of the fundamentals of the reproducing kernel particle method (RKPM) for solving bulk metal forming problems.

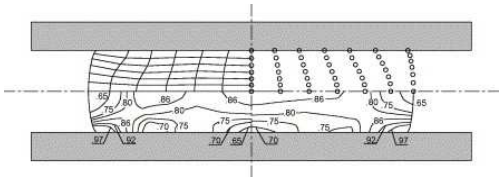

Fig.4 Computed results for the compression of cylindrical performs at 57% height reduction. (Top) Effective stress distribution(MPa) predicted by FEM (left) and RKPM (right). (Bottom) Average stress distribution (MPa) predicted by FEM (left) and RKPM (right).

1. Details of computer implementation are included in the presentation and a new approach based on the rigid-plastic formulation for slightly compressible material models is proposed for simulating two-dimensional non-steady state processes.
2. The validity and efficiency of the proposed RKPM approach for three-dimensional bulk metal forming processes were tested by comparing numerical predictions obtained from a special purpose computer program developed by the authors with finite element calculations.
3. The experimental tests included in the presentation were designed to cover the basic flows and states of stress and strain that are commonly found in two-dimensional bulk forming operations. Data are presented for a wide range of variables such as material flow, geometry and forming load.
4. A numerical example consisting of plane-strain backward extrusion is also included to test the validity of the proposed RKPM approach under large deformations and show its advantage over FEM. Good agreement between RKPM predictions, FEM calculations and experiments confirms the usefulness of the new approach for the simulation of

two-dimensional bulk forming process.

References

1. J. Rojek, O. C. Zienkiewicz and E. Postek, "Advances in FE Explicit Formulations for Simulation of Metal Forming Processes," J. Mater. Process. Tech., Vol. 119, pp.41-47, 2001.
2. O. C. Zienkiewicz, R. C. Taylor and A. Nithiarasu," The Finite Element Method," Vol. 3, 6th Ed., Elsevier.
3. J. S. Chen, C. Pan and C. T. Wu, "Large Deformation Analysis of Rubber based on Reproducing Kernel Particle Method," Comput. Mech., Vol. 19 , pp.211–227, 1997.
4. S. P. Yoon, C. T. Wu, H. P. Wang and J. S. Chen," Efficient Meshfree Formulation for Metal Forming Simulations," ASME, Vol.123, pp.462-467, 2001.
5. S. P. Yoon and J. S. Chen, "Accelerated Meshfree Method for Metal Forming Simulation," Finite Element Analysis, Vol.38, pp.937-948, 2002.
6. A. T. Male and M. G. Cockcroft, " A Method for the Determination of the Coefficient of Friction of Metals under Conditions of Bulk Plastic Deformation," J. Inst. Met. Vol. 93, pp.38–46, 1996.
7. W. K. Liu, S. Jun, S. Li, J. Adee and T. Belytschko," Reproducing Kernel Particle Methods for Structural Dynamics," Int. J. Numer. Methods Eng., Vol. 38, pp.1655-1679, 1995.
8. T. Belytschko, Y.Y Lu and L Gu, "Element Free Galerkin Methods," Int J. Numer. Methods Eng., Vol. **37**, pp.229–256, 1994.
9. D. W. Jung and J. S. Hwang, " A Study of Forming Analysis by using Dynamic- Explicit Finite Element Method in Auto-Body Stamping," J. KSMPE, Vol.3, No.4, pp.63-72, 2004.